

Self-Complementary Adeno-Associated Virus–Mediated Interleukin-1 Receptor Antagonist Gene Delivery for the Treatment of Osteoarthritis: Test of Efficacy in an Equine Model

Rachael S. Watson Levings,¹ Andrew D. Smith,² Ted A. Broome,² Brett L. Rice,² Eric P. Gibbs,¹ David A. Myara,¹ E. Viktoria Hyddmark,¹ Elham Nasri,¹ Ali Zarezadeh,¹ Padraic P. Levings,¹ Yuan Lu,¹ Margaret E. White,¹ E. Anthony Dacanay,¹ Gregory B. Foremny,¹ Christopher H. Evans,³ Alison J. Morton,² Mathew Winter,⁴ Michael J. Dark,⁵ David M. Nickerson,⁶ Patrick T. Colahan,^{2,†} and Steven C. Ghivizzani^{1,*,†}

Departments of ¹Orthopedics and Rehabilitation, ²Large Animal Clinical Sciences, ⁴Small Animal Clinical Sciences, ⁵Infectious Diseases and Pathology, and ⁶Statistics and Actuarial Science, University of Florida, Gainesville, Florida; and ³Rehabilitation Medicine Research Center, Mayo Clinic, Rochester, Minnesota.

†These authors contributed equally to this work as senior authors.

The authors are investigating self-complementary adeno-associated virus (scAAV) as a vector for intra-articular gene-delivery of interleukin-1 receptor antagonist (IL-1Ra), and its therapeutic capacity in the treatment of osteoarthritis (OA). To model gene transfer on a scale proportional to the human knee, a frequent site of OA incidence, studies were focused on the joints of the equine forelimb. Using AAV2.5 capsid and equine IL-1Ra as a homologous transgene, a functional ceiling dose of $\sim 5 \times 10^{12}$ viral genomes was previously identified, which elevated the steady state levels of eqIL-1Ra in synovial fluids by >40-fold over endogenous production for at least 6 months. Here, using an osteochondral fragmentation model of early OA, the functional capacity of scAAV.IL-1Ra gene-delivery was examined in equine joints over a period of 12 weeks. In the disease model, transgenic eqIL-1Ra expression was several fold higher than seen previously in healthy joints, and correlated directly with the severity of joint pathology at the time of treatment. Despite wide variation in expression, the steady-state eqIL-1Ra in synovial fluids exceeded that of IL-1 by >400-fold in all animals, and a consistent treatment effect was observed. This included a 30–40% reduction in lameness and $\sim 25\%$ improvement in total joint pathology by both magnetic resonance imaging and arthroscopic assessments, which included reduced joint effusion and synovitis, and improved repair of the osteochondral lesion. No vector-related increase in eqIL-1Ra levels in blood or urine was noted. Cumulatively, these studies in the equine model indicate scAAV.IL-1Ra administration is reasonably safe and capable of sustained therapeutic IL-1Ra production intra-articularly in joints of human scale. This profile supports consideration for human testing in OA.

Keywords: osteoarthritis, gene therapy, arthritis, AAV, IL-1Ra, osteoarthritis gene therapy

INTRODUCTION

OSTEOARTHRITIS (OA) IS A painful degenerative joint disease marked by gradual persistent erosion of the articular cartilage, subchondral bone sclerosis, osteophyte formation, synovitis, and joint effusion.¹ Although existing medications can reduce joint pain, they cannot inhibit the degradative processes that drive OA, and many patients progress to dis-

abling joint failure, requiring prosthetic joint replacement to regain mobility.

While joint injury and traumatic loading are considered initiating factors in OA, a consensus in the literature points to interleukin-1 (IL-1), synthesized locally by chondrocytes and synovial cells, as a central mediator of disease progression.^{2,3} Although proteins, such as interleukin-1 receptor

*Correspondence: Prof. Steven C. Ghivizzani, Department of Orthopedics and Rehabilitation, University of Florida, P.O. Box 100137, 1600 SW Archer Road, Gainesville, FL 32610. E-mail: ghivisc@ortho.ufl.edu

antagonist (IL-1Ra), can block IL-1 signaling,⁴ conventional methods of drug delivery cannot sustain therapeutic levels intra-articularly.⁵ To overcome this, the authors have been exploring a gene-based treatment for OA whereby the cDNA for *IL-1Ra* is linked to a strong constitutive promoter, packaged in an adeno-associated virus (AAV) vector and injected into the diseased joint.^{6,7} The cells in the articular tissues transduced by the virus continuously synthesize and release transgenic IL-1Ra protein into the local tissues and fluids. Similar gene-based approaches have proven effective for sustained intra-articular protein drug delivery in models of joint disease in a variety of laboratory animals.^{8–10} With respect to the treatment of OA, the AAV vector offers a number of empirical advantages¹¹: (1) the wild-type virus is not associated with human pathology; (2) the vector form does not contain native viral coding sequences, integrates into the target cell genome with low frequency, and has a favorable safety profile in clinical trials⁵; (3) persistent transgenic expression *in vivo* has been observed in many applications^{12,13}; and (4) the small size of the viral particle (~30 nm) allows it to penetrate and transduce cells in dense extracellular matrixes.

In humans, OA frequently develops in the hips and knees—weight-bearing joints that support the body during locomotion.¹⁴ Therefore, following proof-of-principle studies in rabbits, the authors moved to assess the capacity of AAV vectors for *IL-1Ra* gene delivery in an animal model with joints of a clinically relevant scale. The midcarpal and metacarpophalangeal joints of the equine forelimb were targeted,⁷ as they are similar to the human knee in size and function and are likewise highly prone to OA onset.¹⁵ Using a self-complementary AAV vector (scAAV)^{16,17} and human (*h*)*IL-1Ra* cDNA, a pilot study found several AAV capsid serotypes were capable of mediating efficient gene transfer in the context of the equine joint and elevated steady state hIL-1Ra levels in synovial fluids for several weeks.⁷ Recently, to explore more fully its potential for clinical translation, the authors worked to generate a comprehensive pharmacokinetic profile of intra-articular scAAV gene transfer in the equine joint.¹⁸ To minimize the immune profile of the transduced cell population *in vivo* and maximize protein translation, an scAAV vector containing a codon-optimized cDNA for the equine (*eq*)*IL-1Ra* orthologue was generated. Following packaging in the hybrid AAV2.5 capsid,¹⁹ a series of dosing studies found injection of 5×10^{12} viral genomes (vg) of scAAV.eqIL-1Ra could elevate synovial fluid IL-1Ra content >40-fold over endoge-

nous levels for at least 6 months.¹⁸ Using this dose, and green fluorescent protein (GFP) as a cytologic marker gene, local and systemic dispersion of the scAAV vector and transduced cells were compared following injection into healthy equine joints and those with late-stage, naturally occurring OA. While efficient local gene delivery was seen in both environments, GFP activity appeared markedly higher throughout OA joints, with the most striking increases in eroded articular cartilage. In both healthy and diseased joints, vector was effectively contained in the articular tissues at the site of injection.¹⁸

Herein, the results are described of companion studies designed to assess the functional capacity of IL-1Ra following AAV-mediated gene delivery in the context of a large mammalian joint. Using the equine midcarpal joint, the efficacy of local treatment with 5×10^{12} vg scAAV.eqIL-1Ra in a surgically induced, osteochondral fragmentation (OCF) model of early OA was examined. This model closely simulates the initiation and early progression of natural OA in the horse.²⁰ The effects of treatment were assessed with diagnostic technologies used routinely for human OA, including arthroscopy, magnetic resonance imaging (MRI), and motion analysis, and were correlated with synovial fluid eqIL-1Ra levels over time.

RESULTS AND DISCUSSION

Objectives and study design

Evaluation of scAAV.eqIL-1Ra efficacy in an osteochondral fragmentation model of OA. To assess the functional capacity of scAAV-mediated eqIL-1Ra expression in the equine forelimb joint, an OCF model of OA was used adapted from Frisbie *et al.*²⁰ For this study (diagrammed in Fig. 1a), 20 healthy Thoroughbred horses were randomly assigned to two equal groups: treated and control. In one midcarpal joint of each animal, a small osteochondral lesion was generated arthroscopically at the distodorsal aspect of the radiocarpal bone (Fig. 1b). The contralateral joint received a parallel arthroscopic examination and served as a sham-operated internal control. At 2 weeks post surgery (study day 0), the OCF joint of the horses in the treated group received an injection of 5×10^{12} vg of scAAV.eqIL-1Ra. The OCF joints of the control horses and the sham-operated joints of both groups were injected with an equal volume of the saline vehicle. One week post treatment, the horses were placed on an athletic training schedule for 10 weeks, which, in the context of the osteochondral

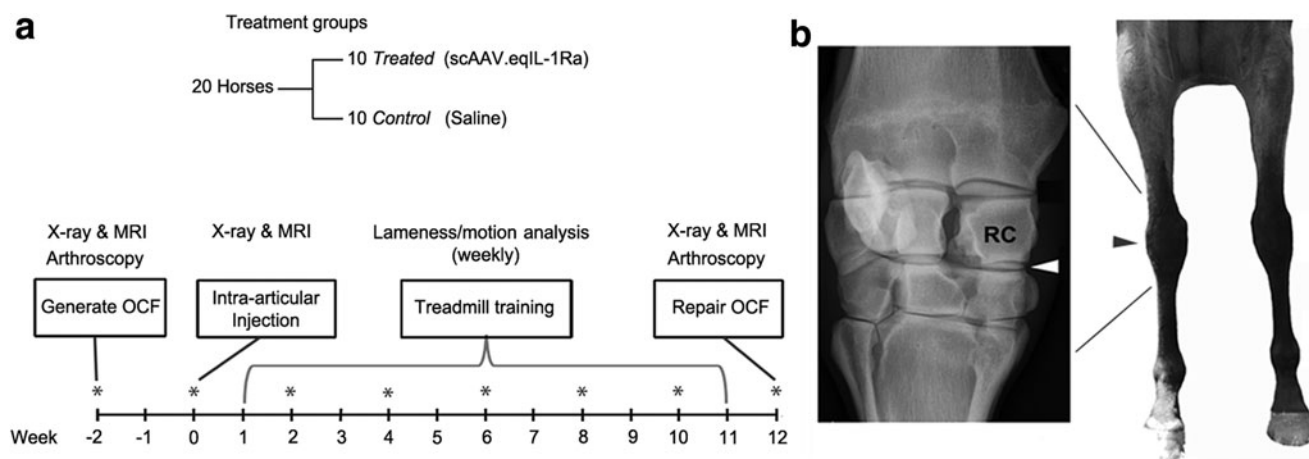


Figure 1. Design of the OCF efficacy study. **(a)** Twenty Thoroughbred horses were randomly divided into equal treated and control groups. Two weeks prior to injection, an arthroscopic examination was performed on both intercarpal joints. In one joint, an 8 mm osteochondral lesion was created medially off the radiocarpal bone. Two weeks later, horses assigned to the treated group received an injection of 5×10^{12} viral genomes (vg) of scAAV.eqIL-1Ra into the joint space of the OCF joint; horses in the control group received an equal volume of Lactated Ringer's solution. One week later, horses began an athletic treadmill training program 5 days a week for 10 weeks. At its conclusion, a final arthroscopic exam was performed on both intercarpal joints. The fragment was removed and the lesion repaired. Radiographic imaging and MRI were performed immediately prior to both arthroscopic surgeries and prior to treatment at week 0. Digital images were collected during both arthroscopic procedures. Synovial fluids from both intercarpal joints, as well as peripheral blood and urine, were collected immediately before treatment and on alternate weeks throughout the protocol (*). During treadmill training, the horses were evaluated weekly for lameness by both visual scoring and motion analysis. **(b)** *Left:* Radiographic image of an equine carpal joint. The *white arrowhead* indicates the intercarpal joint. *Right:* Anatomic location of the carpal joint on the equine forelimb. The *black arrowhead* indicates the position of the intercarpal joint. scAAV.eqIL-1Ra, self-complementary adeno-associated virus carrying interleukin-1 receptor antagonist cDNA; MRI, magnetic resonance imaging; OCF, osteochondral fragment; RC, radiocarpal bone (site of the osteochondral lesion).

injury, induces pathologies consistent with early-stage OA.²⁰

At the conclusion of the training period, the midcarpal joints of the animals were examined arthroscopically, and the osteochondral fragment and adjacent synovium were collected for analysis. The lesion was debrided and repaired, and following recovery, the animals were returned to the research herd. Digital images were collected during both arthroscopic procedures. Radiographic imaging and MRI were performed immediately prior to both arthroscopic procedures (weeks -2 and 12) and prior to treatment at week 0. Weekly during the training period, the horses were evaluated for forelimb lameness. Peripheral blood, urine, and synovial fluid from both midcarpal joints were collected from each horse immediately prior to intra-articular injection and were used to determine the pretreatment levels of IL-1Ra, capsid-specific neutralizing antibody (NAb), and prostaglandin E₂ (PGE₂), as described. Similar fluids were collected on alternate weeks thereafter for the remainder of the protocol.

Summary of data

Local and systemic eqIL-1Ra levels following vector administration. Compared to pre-injection levels at week 0, enzyme-linked immunosorbent

assay (ELISA) measurement of recovered synovial fluids showed a significant increase in eqIL-1Ra content in the OCF joints of the treated group. Mean eqIL-1Ra levels peaked 2 weeks post injection at ~ 214 ng/mL (Fig. 2a), approximately fourfold higher than previously observed in healthy joints at the same viral dose¹⁸ (indicated by the dashed line in Fig. 2a). Over the course of the training period, eqIL-1Ra expression gradually diminished to ~ 59 ng/mL, similar to that seen with AAV gene transfer in normal joints.¹⁸ eqIL-1Ra in synovial fluids from the control OCF joints, as well as the sham-operated joints of both groups, remained at pretreatment levels (<1 ng/mL) throughout. Although the mean eqIL-1Ra levels in the treated joints showed a reasonably consistent trend over time (Fig. 1a), transgene expression among the individual animals varied considerably (Fig. 2b), especially at week 2, where eqIL-1Ra levels among the treated animals ranged >230 -fold and in one animal were >930 ng/mL. By the end of the study, much of the early variation had resolved, and the range in eqIL-1Ra narrowed to ~ 30 -fold, with the highest expression at 119 ng/ml. Endogenous IL-1 remained below the level of detection (16 pg/mL) in all biological fluids throughout the course of the study.

eqIL-1Ra content in urine and peripheral blood serum was measured to assay for leakage of

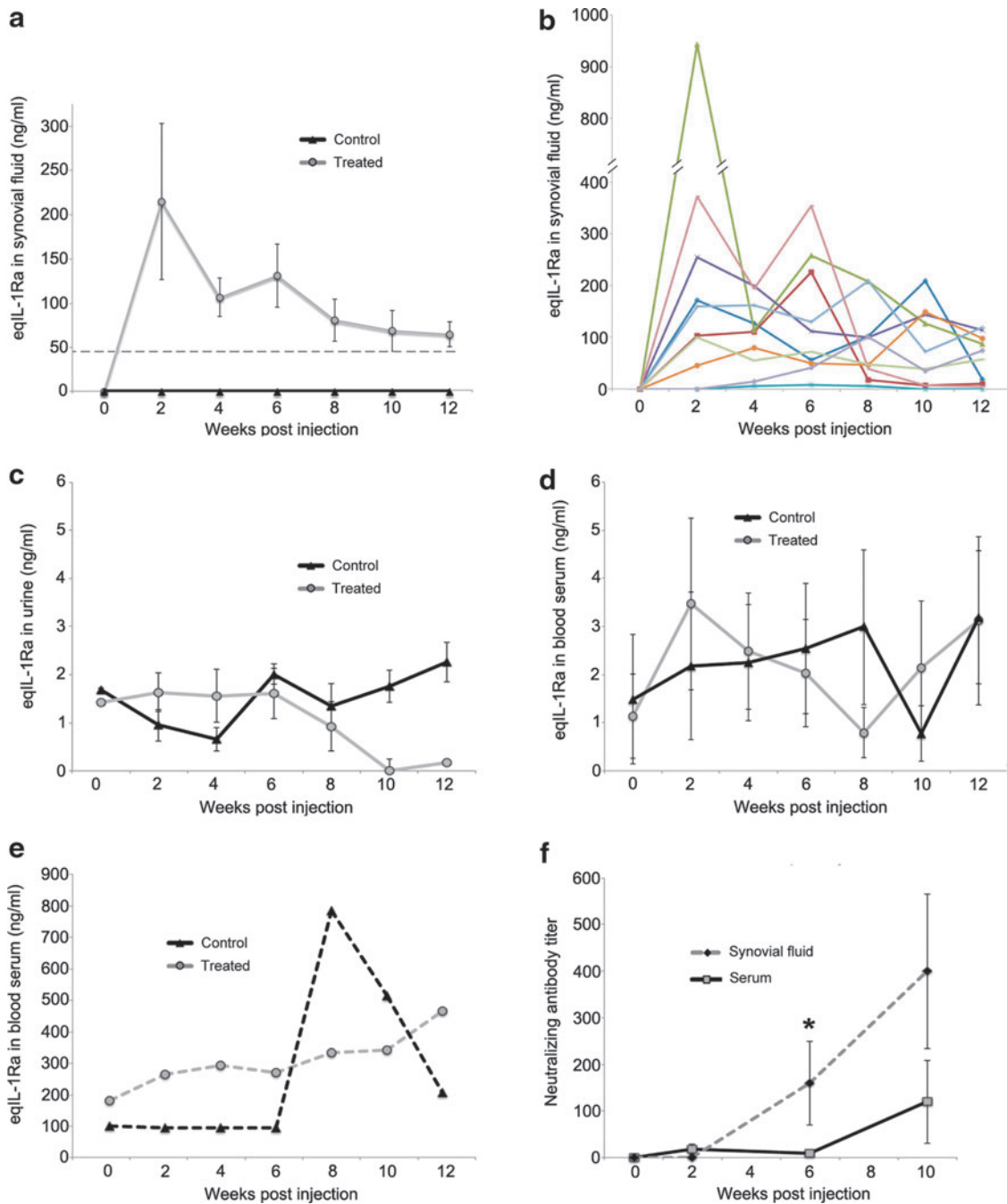


Figure 2. eqIL-1Ra content and AAV2.5 neutralizing antibody (NAb) in recovered biological fluids. **(a)** Mean eqIL-1Ra levels in synovial fluid of the OCF joints from the treated and control groups ($n=10$). The *dashed line* reflects mean AAV.eqIL-1Ra expression in healthy joints from the same viral dose.¹⁵ For **(a–f)**, the week 0 values represent baseline levels in the respective biological fluids collected immediately before injection of vector (treated group) or the Lactated Ringer's solution vehicle (control group) **(b)** Synovial fluid eqIL-1Ra in the OCF joint of the individual horses in the treated group. Each color reflects a different animal. **(c)** Mean eqIL-1Ra in urine for both the treated and control groups ($n=10$). **(d)** Mean eqIL-1Ra in serum from peripheral blood for 9/10 animals in both the treated and control groups. **(e)** eqIL-1Ra in blood serum from the remaining horses (one each from the treated and control groups), which prior to treatment were $>25\times$ greater than the other 18 animals in the study. **(f)** AAV.2.5 NAb titers in synovial fluids of the OCF joints and peripheral blood serum and of the horses in the treated group ($n=10$). Error bars represent \pm standard error of the mean (SEM). * $p<0.05$.

transgenic protein from the joint. In urine, mean eqIL-1Ra levels remained consistently low (<3 ng/mL) with no meaningful differences between groups (Fig. 2c). Similarly, mean eqIL-1Ra in serum remained <4 ng/mL for 9/10 horses in both

groups (Fig. 2d). Prior to injection at week 0 and without obvious cause, one horse from each group showed serum eqIL-1Ra levels >100 ng/mL (Fig. 2e), which, over the course of the protocol, increased to >500 ng/mL. Given the extraordinarily high base-

line levels of IL-1Ra in the sera of both these animals, and the temporal profile of the animal from the control group (never exposed to AAV.eqIL-1Ra), the high serum IL-1Ra levels in the treated animal in Fig. 2e were attributed to endogenous production from causes unrelated to the AAV vector or transgene. Interestingly, despite the increase in circulating levels in both of these animals, no accompanying increase in eqIL-1Ra content was seen in the synovial fluid of the sham-operated joints of either horse, or the OCF joint of the control horse, with each consistently remaining <1 ng/mL.

Consistent with the findings of others,^{12,21,22} an increase was observed in AAV2.5 NAb titer over time in both the blood serum and synovial fluid of the horses receiving the AAV vector (Fig. 2f). Though the NAb titer in synovial fluids from injected OCF joints was consistently several fold

higher than blood, this was only significant at the week 6 time point. Biological fluids from horses in the control group showed no measurable increase in NAb.

Treatment with scAAV.eqIL-1Ra reduces forelimb lameness in the OCF model. To assess the effect of treatment on joint pain, forelimb lameness was evaluated using visual scoring by the AAEP grading scale (Fig. 3a, left panel) and by motion analysis using wireless detection of attached inertial sensors (Fig. 3a, right panel).^{23,24} In both graphics, lameness over time was plotted as the mean percent change relative to the start of training at week 1 post injection. Relative to controls, the treated group showed a gradual but progressive reduction in lameness by both methods, with peak improvement of 36% ($p=0.03$) at week 10 by visual assessment

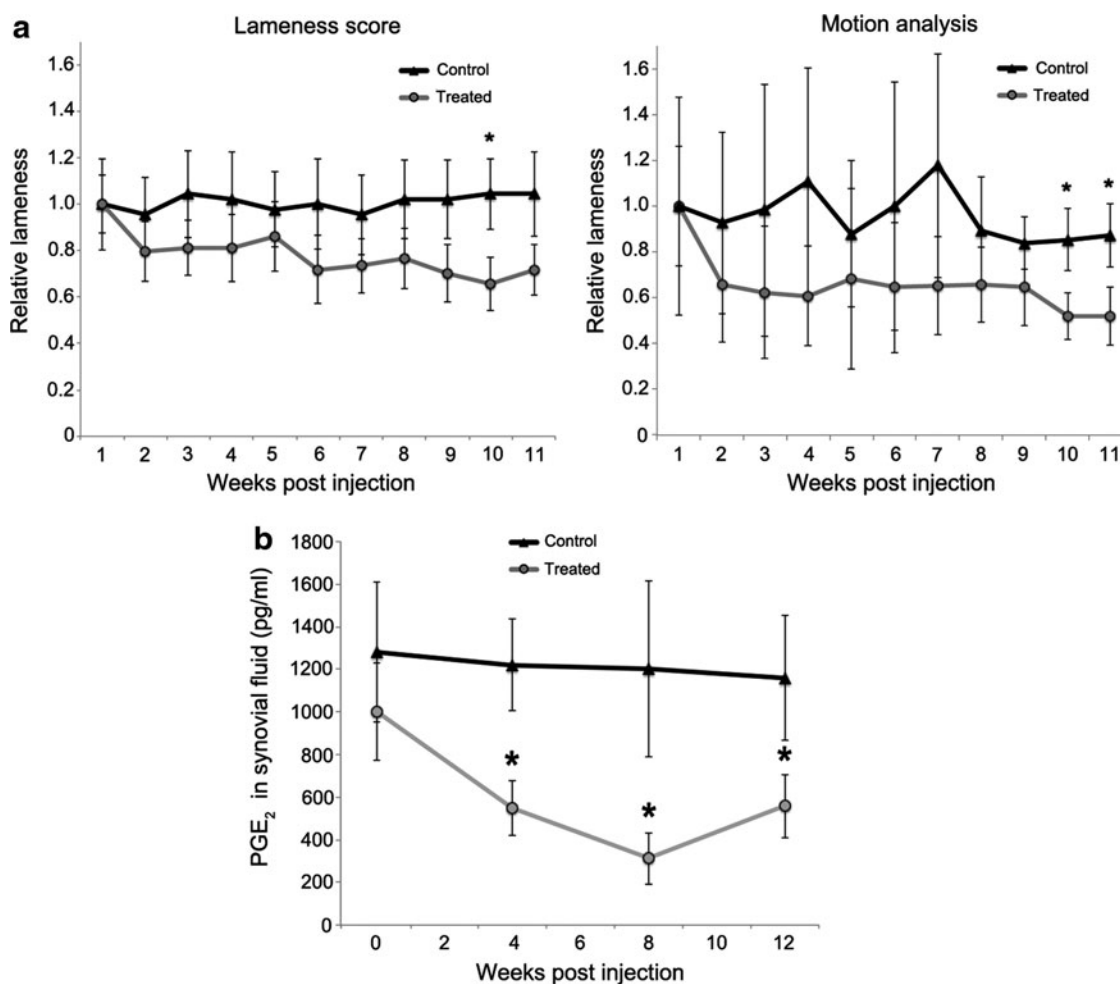


Figure 3. Changes in forelimb lameness and synovial fluid prostaglandin E₂ (PGE₂) following treatment with scAAV.eqIL-1Ra. **(a) Left:** Relative change in mean visual lameness scores between treated and control groups during athletic training. **Right:** Relative change in lameness (vector sum) assessed by the inertial sensor motion analysis system (Lameness Locator[®]). For both, mean lameness scores at week 1 were assigned a value of 1, and subsequent measurements were calculated as percent change. For both types of assessments, the observers were blinded to the treatment of the animals throughout the experimental protocol. **(b)** Mean PGE₂ levels in synovial fluid of OCF joints of both the treated and control groups. Error bars represent SEM. * $p < 0.05$.

and $\sim 40\%$ ($p=0.04$) at weeks 10 and 11 by motion analysis. In agreement with these functional indexes, PGE₂ content in joint fluids was reduced by $>50\%$ in the treated group over controls from week 4 through the conclusion of the protocol (Fig. 3b).

scAAV.eqIL-1Ra delivery reduces inflammation and enhances repair of the osteochondral injury. Although radiographic abnormalities were seen in all OCF joints at 2 weeks post surgery and at the endpoint,

the anatomic complexity of the carpal joint coupled with position variability between imaging sessions prevented uniform temporal comparisons among horses. MRI, however, provided a clearer representation of the pathologic changes in the joint, allowing comparison of pretreatment (week 0) and endpoint scores (week 12) for each individual^{25,26} (Fig. 4). In all cases, the changes in the MR images were primarily found medially, in the vicinity of the surgically generated fracture. At 2 weeks post

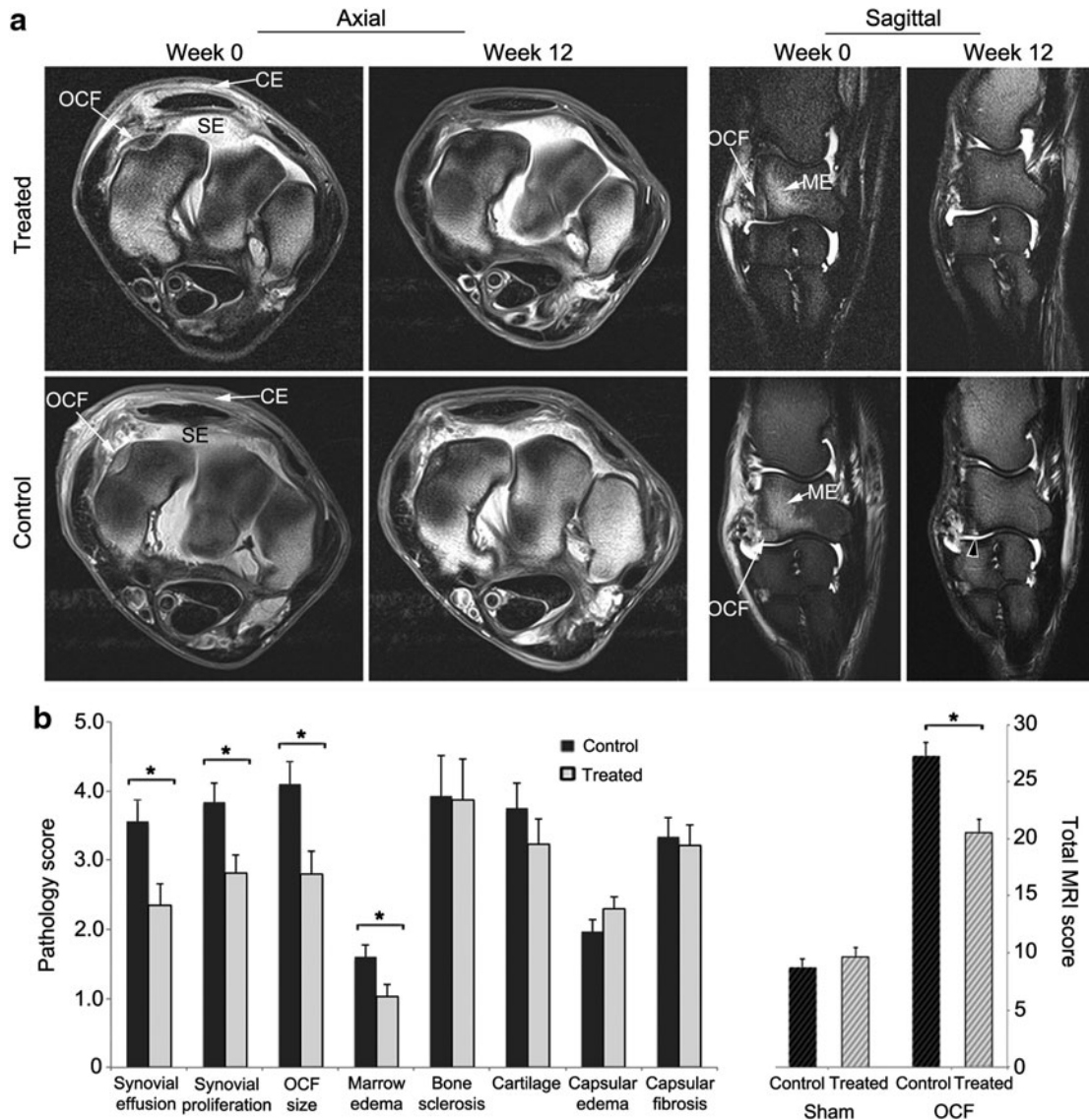


Figure 4. Evaluation of MR images for changes in tissue pathology in OCF joints treated with scAAV.eqIL-1Ra. Both carpal joints of the horses in the treated and control groups were scanned by MRI immediately prior to treatment (week 0) and at the end of the experimental protocol (week 12). From these scans, trained observers blinded to the identity of the horses and their treatment scored both joints for synovial effusion, synovial proliferation, the severity of the osteochondral lesion (OCF size), marrow edema in the radiocarpal bone, sclerosis of the radial carpal and third carpal bones, and joint capsule edema and fibrosis on a scale from 0 to 10, where 0=normal and 10=severe pathology. **(a)** Images from axial and sagittal scans (PD and PD-FS, respectively) of OCF joints from representative horses in the treated and control groups. *White arrows* indicate: CE, capsular edema; ME, marrow edema; OCF, osteochondral fragment; SE, synovial effusion. *Black arrow* in week 12 sagittal scan for the control joint indicates hyperintense signal and incomplete OCF repair. **(b)** *Left:* Covariate analyses of the major joint pathologies associated with the OCF model in treated and control groups at the endpoint (week 12) using the pretreatment scores (week 0) as baselines. *Right:* Total MRI scores for the OCF joints were calculated from the values of the individual MRI pathologies. Total MRI scores from sham-operated joints represent baseline pathology in contralateral intercarpal joints. Error bars represent \pm SEM. * $p < 0.05$. PD, proton density; PD-FS, proton density with fat suppression.

injury (study week 0), a well-defined high-intensity signal delineated the boundaries of each fragment in the radial carpal bone, and was accompanied variably by increased density of the adjacent bone, regional fluid accumulation in the marrow (marrow edema), synovial effusion, and hyperplasia, as well as fibrotic expansion and edema of the joint capsule.^{26,27} Using the pretreatment scores (week 0) for these pathologies as baselines for each horse, an analysis of covariance was performed with the scores from MRI scans acquired at the endpoint in order to assess the effects of treatment on joint morphology. As reflected in Fig. 4, both groups

showed equivalent changes in the joint capsule, with reduced capsular edema and increased fibrotic thickening, which were attributed primarily to the arthroscopic procedure and fluid infusion and less to the osteochondral lesion. Consistent with the anti-inflammatory properties of IL-1Ra, the OCF joints in the treated group showed significantly reduced joint effusion (34%; $p=0.008$) and synovial proliferation (27%; $p=0.008$) relative to controls (Fig. 4b). The treated group also showed a 32% ($p=0.01$) improvement in fracture repair and a 36% ($p=0.02$) reduction in marrow edema. Across the major pathologies induced by the OCF, the

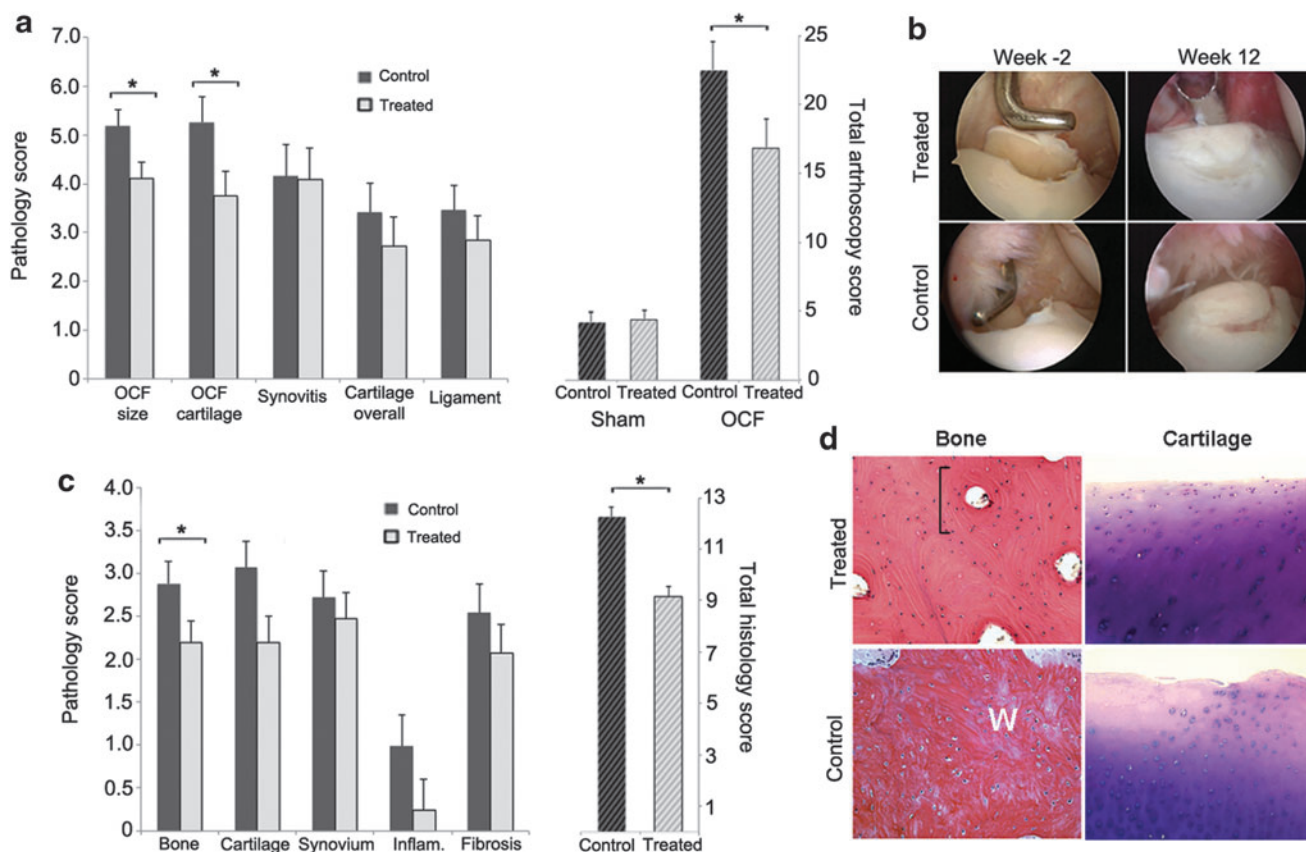


Figure 5. Evaluation of OCF joint arthroscopies and histologic sections for changes in tissue pathology associated with scAAV.eqIL-1Ra treatment. Both intercarpal joints of the horses in the treated and control groups were examined arthroscopically immediately before and after generation of the osteochondral lesion (week -2), and then at the endpoint (week 12) prior to removal of the fragment and local debridement. Video recordings and digital images collected during the procedures were scored by trained observers (blinded to the identity of the animals and their treatment groups) for OCF size and local cartilage damage, synovitis, cartilage damage throughout the joint (overall), and inflammation of tissue ligament-associated tissues. During the final arthroscopic procedure, the osteochondral fragment and regional synovial tissue were removed, sectioned and stained with hematoxylin and eosin (H&E) or toluidine blue, and graded by observers blinded to the identity of the donor animal. **(a) Left:** Covariate analyses of arthroscopic assessments of the major joint pathologies associated with the OCF model in treated and control groups at week 12 using the post-fracture scores at week -2 as baseline. **Right:** Total arthroscopy scores for the OCF joints were calculated from the values of the individual pathologies. Total scores from sham-operated opposing intercarpal joints represent baseline pathology in uninjured joints. Error bars represent \pm SEM. $*p < 0.05$. **(b)** Representative arthroscopic images of the osteochondral lesions in treated and control horses at the time of generation (week -2) and at the endpoint (week 12). **(c) Left:** Mean histologic scores for individual tissue pathologies in collected OCF tissues. **Right:** Total histologic scores calculated from the individual tissue scores. Error bars represent \pm SEM. $*p < 0.05$. **(d)** Representative microscopic images of bone repair tissue (H&E) and cartilage (toluidine blue) in treated and controls as indicated. **Top left:** Lamellar bone with small osteocytes, interstitial lamellae and osteons with concentric lamellae surrounding haversian canals (*bracket*). **Bottom left:** Woven bone (*W*) with randomly organized collagen fibers and large osteocytes in lacunae distributed irregularly in the direction of the collagen fibers. **Top right:** Articular cartilage with small flat chondrocytes in the superficial layer transitioning to mildly hypertrophic chondrocytes in radial columns in the deeper layer. **Bottom right:** Articular cartilage with mild surface irregularity and an acellular focus to the left. Chondrocytes in the superficial layer show signs of hypertrophy and disorientation.

treated joints showed a 25% ($p=0.001$) reduction in total pathologic score relative to controls (Fig. 4b).

Arthroscopic images taken immediately before and after generation of the osteochondral lesion, and again at the endpoint (prior to surgical repair of the fragment), were also blindly scored for pathologies (Fig. 5a and b). Covariate analyses were performed using the pretreatment scores (week -2) as baselines. The results were largely consistent with those from the MRI. Animals in the treated group showed significantly improved repair of the osteochondral lesion (29%; $p=0.03$) and maintenance of the articular cartilage adjacent to the fracture (17%; $p=0.02$). Although there were trends toward improvement in the global cartilage scores and ligament inflammation, these did not achieve statistical significance individually. Cumulatively, however, across all pathologic parameters, the treated OCF joints showed 24% ($p=0.04$) improvement in total

arthroscopic pathology scores. In agreement with these data, in 8/10 horses in the treated group, the osteochondral lesions had repaired to the extent that they required a chisel for removal of the fragment originally created. Conversely, in 7/10 horses in the control group, the repair tissue was spongy and soft by indentation, and the fragment was easily removed with arthroscopic forceps.

Histologic examination of the recovered fragments and adjacent synovial tissues showed significant differences in the quality of the repair bone at the boundary of the OCF lesion (Fig. 5c and d). Consistent with the findings from arthroscopy and MRI, in the treated group, the bony tissue at the interface appeared more mature, with greater mineralization and formation of lamellar bone with defined osteons (Fig. 5d). The repair tissue in the control group was mainly comprised of primary woven bone (Fig. 5d). Although there was a strong

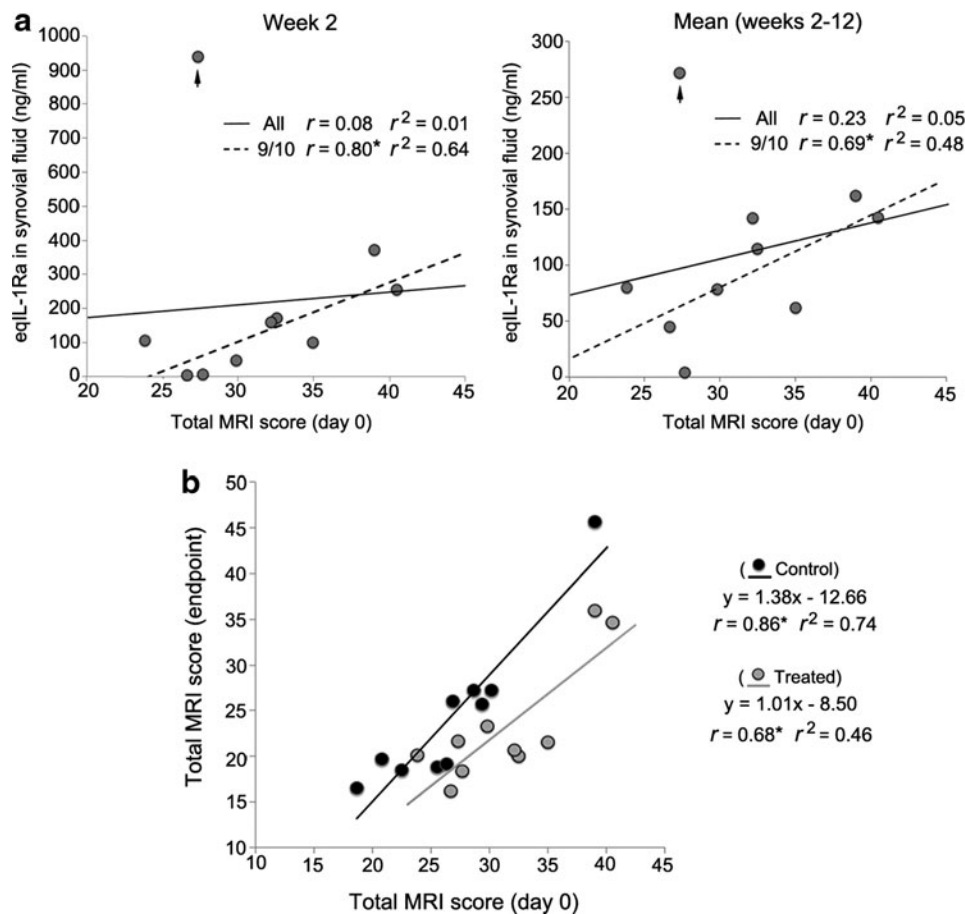


Figure 6. Associations between transgenic eqL-1Ra expression and joint pathology in the OCF model. **(a)** Plots of total MRI score in the OCF joints of the treated horses at week 0 versus *(left)* synovial fluid eqL-1Ra levels at week 2, and *(right)* eqL-1Ra levels averaged from weeks 2–12. For both plots, the arrow designates the data point from one horse with unusually high eqL-1Ra expression at week 2 relative to the other nine animals (see Fig. 1c). The solid lines show the best-fit line plots for the data points of all 10 animals. The dashed lines show the best-fit line plots calculated without the outlying data point (9/10) are shown. Pearson correlation coefficients (r) for MRI score and eqL-1Ra levels both with (all) and excluding the outlying data point (9/10) are shown. **(b)** Plot of total MRI scores at week 0 versus total MRI score at week 12 for the OCF joints of each horse in the treated (gray) and control (black) groups. The solid lines show the respective best-fit line plots for each group. The corresponding line equations and Pearson correlation coefficients (r) are also shown as indicated. * $p < 0.05$.

trend toward improved cartilage, the scores fell just outside the range for statistical significance ($p=0.06$). Modest reductions in mean scores for synovial infiltration and fibrosis were also observed, but these also were not statistically significant. By the criteria evaluated, the treated joints showed $\sim 24\%$ ($p=0.003$) improvement in total pathologic score relative to the untreated controls (Fig. 5c).

Associations between joint pathology, eqIL-1Ra expression, and therapeutic effect. Having previously seen markedly increased AAV transgene expression in joints with naturally occurring late-stage OA, relative to healthy joints,¹⁸ the study looked in the treated group for an association between intra-articular eqIL-1Ra expression and the severity of joint pathology at the time of injection. For each of the treated animals, the total MRI pathology scores at week 0 were compared to: (1) peak synovial fluid eqIL-1Ra levels at week 2 post injection (Fig. 6a, left panel), and (2) eqIL-1Ra expression averaged over the course of the study (Fig. 6a, right panel). However, no significant correlation was noted. If, though, the horse with eqIL-1Ra expression of 930 ng/mL at week 2 is considered an outlier, among the nine remaining animals, a strong direct correlation is seen between joint pathology at injection and eqIL-1Ra produced at week 2 ($r=0.80$; $p=0.01$), as well as eqIL-1Ra levels averaged across all time points ($r=0.69$; $p=0.03$). Thus, for 90% of the animals in the treated group, there was a significant direct association between the severity of joint pathology at the time of treatment and the amount of transgenic IL-1Ra subsequently produced in the joint.

Interestingly, although synovial fluid eqIL-1Ra levels over the 10-week study ranged more than 25-fold among the individual horses in the treated group, we saw no significant association with the level of eqIL-1Ra produced and therapeutic benefit. A plot of the total MRI pathology scores of the OCF joints of all 20 horses immediately prior to injection versus the total MRI score at endpoint (Fig. 6b) illustrates the effect of treatment with AAV.eqIL-1Ra relative to control joints injected with saline. Using the formulas for the best-fit lines for the data points of the respective treated and control groups, a consistent 24–25% improvement with scAAV.eqIL-1Ra treatment is estimated, regardless of the severity of the starting pathology (Fig. 6b). Considering the high variability in eqIL-1Ra expression in the OCF joints of the treated animals (Figs. 2b and 6a and b), these data suggest that each of the joints receiving scAAV.eqIL-1Ra achieved the maximum level of efficacy in this model system.

CONCLUSIONS

Altogether, these data show that in joints proportional in size to the human knee, local AAV gene transfer can provide persistent IL-1Ra transgene expression at therapeutically relevant levels. Despite variable expression among treated joints in the context of an acute osteochondral lesion, the sustained increase in eqIL-1Ra content following a single injection of AAV vector provided meaningful benefit, resulting in reduced joint lameness and intra-articular PGE₂, improved repair of the damaged bone, and protection of the adjacent cartilage. No adverse response to the vector or transgene was observed in the disease model, and at least within the equine system, intra-articular overexpression of IL-1Ra provided no apparent risk of immunosuppression from systemic IL-1 blockade.

Similar to previous reports,²¹ an increase in AAV2.5 NAb titer was observed in both synovial fluid and blood serum following intra-articular vector delivery. While the capsid-directed humoral response had no obvious effect on transgene expression, its impact on the efficacy of subsequent vector treatments is uncertain. Although pre-existing NAb is a potential concern with the use of AAV vectors, there is evidence that vector neutralization can be averted with the use of serologically distinct AAV capsids.²⁸ It's also possible that simple joint lavage prior to treatment will transiently reduce the local NAb titer to permit effective vector delivery. Considering the apparent efficiency of AAV transduction in articular chondrocytes in OA cartilage^{10,18} and the low rate of chondrocyte turnover *in vivo*, sustained gene-mediated chondroprotection may be achievable without frequent vector administration.

In addition to measuring capsid-specific NAb, future studies will include assessment of T-cell activation to the AAV vector capsid and transgene prior to vector administration and at time points downstream using ELISpot assays. Considering the problems from pre-existing cellular immunity to capsid protein in clinical trials of AAV gene therapy, an understanding of the influence of both cellular and humoral immunity on intra-articular AAV gene transfer and transgenic expression will be important for the development of successful treatment protocols and for patient selection for clinical trials.

OA pathology enhances intra-articular transgene expression

Conventional methods of drug delivery provide the practitioner with a reasonable degree of control, in that a defined dose can be administered to achieve a predictable, though transient, effect. In

the current paradigm, cells in the articular tissues are genetically modified with a virus to synthesize and secrete IL-1Ra protein continuously into the joint space and local tissues. However, as the amount of transgenic protein produced at any particular time reflects the collective synthesis of the modified cells present in the joint, drug levels can vary widely (both within and among individuals) based on the nature of the cell populations encountered by the vector at the time of administration and subsequent changes in their number, composition, and activation over time.

Recent data show that the increased cellularity and the pathologic changes in the OA tissues can increase intra-articular transgene expression substantially.¹⁸ Further, the CMV promoter used to drive the scAAV expression cassette is highly responsive to stress and inflammatory activation in the pathologic environment. Consistent with this, AAV.eqIL-1Ra delivery into inflamed joints with an acute osteochondral injury resulted in an approximately fourfold increase in transgenic IL-1Ra expression over that seen in healthy joints. Although transgenic IL-1Ra in synovial fluid ranged >100-fold among the OCF joints at 2 weeks post treatment, in 9/10 animals, there was a strong direct correlation between the severity of joint pathology (total MRI score) at the time of vector injection and the level of expression of the IL-1Ra transgene. Moreover, coincident with the resolution of the acute inflammation and healing of the fracture over time, the unusually high transgenic IL-1Ra expression likewise gradually diminished and, at the week 12 endpoint, approached levels produced in normal joints.

Utility of IL-1Ra as a therapeutic gene in OA

In joints treated with scAAV.eqIL-1Ra, a mean improvement in overall pathology of ~25% was observed relative to controls. Consistent with its role as an anti-inflammatory,²⁹ sustained overexpression of eqIL-1Ra reduced joint effusion and synovitis and, in the latter weeks of the study, significantly improved mobility. Although there was evidence of chondroprotection in the cartilage adjacent to the lesion, the effect was not joint-wide. In this acute injury model, cartilage degeneration distal to the osteochondral lesion was modest, making any changes due to treatment difficult to detect.

Naturally occurring OA is insidious and typically follows a gradual progression over months and years following primary injury. While the short-term effects of *IL-1Ra* gene delivery in the context of an acute injury may appear somewhat

modest relative to other treatments, such as corticosteroid injection, the advantages of the gene-based approach, however, lie in the capacity to provide sustained protein drug delivery following a single injection (for at least 6 months) and the ability to administer biological agents with disease-modifying activity. Along these lines, the differences in joint lameness only reached statistical significance late in the study after the acute inflammatory phase of the osteochondral injury had largely resolved. It is envisioned that the effects of treatment will be more evident with the passage of time. To address this directly and to determine the long-term effects on repair, efficacy, and safety, the efficacy and safety of local scAAV.eqIL-1Ra delivery is currently being investigated in a chronic OA model over a 12-month time frame, where it is hypothesized that sustained IL-1Ra expression will lead to a more distinct chondroprotective effect. It is expected that sustained IL-1 inhibition will provide cumulative benefit and become more pronounced with increasing time post treatment.

Interestingly, despite a reduction in synovial fluid PGE₂, the treated group showed significantly improved repair of the osteochondral fracture relative to controls. This finding appears to conflict with the literature, indicating vital roles for cyclooxygenase-2 and the prostaglandins in fracture repair.^{30,31} These molecules, though, primarily contribute to the acute inflammatory phase of bone healing, which begins to resolve around 7–14 days post injury, giving way to repair processes of cellular differentiation and matrix synthesis.³² While acute inflammation is required to initiate the repair process, persistent inflammation can impede activation of the Wnt/ β -catenin pathway and osteoblast differentiation, which inhibits bone repair.^{33,34} Therefore, by administering the vector at 2 weeks post surgery, the reduced inflammatory signaling from IL-1Ra overexpression likely served to enhance osteoblast differentiation during the repair phase, leading to improved healing. Along these lines, treatment with AAV.IL-1Ra in a similar time frame post joint injury may provide therapeutic/prophylactic benefits in post-traumatic OA, combining reduced inflammation and enhanced tissue repair with potential downstream chondroprotection.

Although intra-articular transgene expression occurred over a wide range, no correlation was found between synovial fluid eqIL-1Ra content and therapeutic benefit. This is attributed to the mode of action of IL-1Ra as a competitive inhibitor of the IL-1 type 1 receptor.⁴ Due to the potency of IL-1 signaling, IL-1Ra must be present in 100- to 1,000-

fold excess over IL-1 to completely inhibit its activity.^{35,36} In the OCF joints, synovial fluid IL-1 was below the limit of detection (16 pg/mL). Thus, in the majority of treated joints, IL-1Ra was present in a 6,000-fold excess, and at least a 400-fold excess in the joints with the lowest expression. As IL-1Ra has no known agonist effect,⁴ once the available IL-1 receptors are saturated, additional IL-1Ra can provide no further benefit. Considering these points, the consistent ~24–25% improvement in joint pathology observed across the treated group likely reflects the maximum benefit achievable in this disease model with this method of IL-1Ra delivery.

Overall, IL-1Ra appears well-suited to intra-articular gene therapies for OA. It does not require sophisticated regulation, and once the therapeutic threshold is achieved, overproduction has little apparent adverse consequence. Although likely beneficial, the data indicate that *IL-1Ra* gene delivery is unlikely to be a cure for OA. To expect otherwise would be unrealistic. IL-1Ra is only capable of blocking the IL-1 signaling component of OA, an extremely complex disease that involves large-scale pathologies and processes mediated at the level of the tissues and the organism. Nonetheless, as IL-1 is a primary driver of the inflammatory cascade and plays an active role in the majority of erosive processes mediated at the cellular level, it has the potential to provide meaningful benefit to patients over a broad spectrum of disease severity.

Altogether, the data from this study demonstrate that a gene-based therapy using recombinant AAV can provide persistent, effective delivery of an anti-arthritic protein to joints of human proportion. Moreover, AAV.IL-1Ra applied soon after joint injury can reduce pathologic development in an acute model of pre-OA. Based on the cumulative findings of the authors' recent studies in the equine system, AAV.IL-1Ra combines therapeutic

efficacy with minimal apparent biosafety risk and thus provides a profile supportive of clinical testing in human and equine OA. The Materials and Methods section can be found in the Supplementary Data (available online at www.liebertpub.com/humc).

ACKNOWLEDGMENTS

This project was supported by grants AR048566 and AR048566-S from the National Institute of Arthritis Musculoskeletal and Skin Diseases (NIAMS) of the National Institutes of Health. We acknowledge Lorraine Matheson and the National Gene Vector Biorepository for assistance in obtaining the packaging/helper plasmids for the AAV2.5 capsid, and MaryBeth Horodyski, Darlene Bailey, and Jennifer Streshyn for administrative assistance. We also acknowledge the facilities that assisted with large scale preparation of the AAV vectors for the study: (1) the Vector Core of the Powell Gene Therapy Center at the University of Florida with assistance from Mark Potter, and (2) the Vector Core of the University of North Carolina at Chapel Hill with patient assistance from Josh Grieger.

The optimized equine *IL-1Ra* cDNA can be obtained from the corresponding author through material transfer agreement with the University of Florida. The pXR.2.5, pXX6-80, and pHpa-tr-SK (ScAAV-CMV-GFP) plasmids for packaging self-complementary vectors in the AAV2.5 capsid are available through the National Gene Vector Biorepository and material transfer agreement with the University of North Carolina at Chapel Hill.

AUTHOR DISCLOSURE

C.H.E. and S.C.G. are inventors on several patents and patent applications describing cell- and gene-based therapies for arthritis and connective tissue disorders.

REFERENCES

- Loeser RF, Goldring SR, Scanzello CR, et al. Osteoarthritis: a disease of the joint as an organ. *Arthritis Rheum* 2012;64:1697–1707.
- Olson SA, Horne P, Furman B, et al. The role of cytokines in posttraumatic arthritis. *J Am Acad Orthop Surg* 2014;22:29–37.
- Kapoor M, Martel-Pelletier J, Lajeunesse D, et al. Role of proinflammatory cytokines in the pathophysiology of osteoarthritis. *Nat Rev Rheumatol* 2011;7:33–42.
- Arend WP, Malyak M, Guthridge CJ, et al. Interleukin-1 receptor antagonist: role in biology. *Annu Rev Immunol* 1998;16:27–55.
- Chevalier X, Goupille P, Beaulieu AD, et al. Intra-articular injection of anakinra in osteoarthritis of the knee: a multicenter, randomized, double-blind, placebo-controlled study. *Arthritis Rheum* 2009;61:344–352.
- Kay JD, Gouze E, Oligino TJ, et al. Intra-articular gene delivery and expression of interleukin-1Ra mediated by self-complementary adeno-associated virus. *J Gene Med* 2009;11:605–614.
- Watson RS, Broome TA, Levings PP, et al. scAAV-mediated gene transfer of interleukin-1 receptor antagonist to synovium and articular cartilage in large mammalian joints. *Gene Ther* 2013;20:670–677.
- Evans CH, Ghivizzani SC, Robbins PD. Arthritis gene therapy and its tortuous path into the clinic. *Transl Res* 2013;161:205–216.

9. Madry H, Cucchiari M. Advances and challenges in gene-based approaches for osteoarthritis. *J Gene Med* 2013;15:343–355.
10. Goodrich LR, Grieger JC, Phillips JN, et al. scAAVIL-1ra dosing trial in a large animal model and validation of long-term expression with repeat administration for osteoarthritis therapy. *Gene Ther* 2015;22:536–545.
11. Goater J, Muller R, Kollias G, et al. Empirical advantages of adeno associated viral vectors *in vivo* gene therapy for arthritis. *J Rheumatol* 2000;27:983–989.
12. Mason JB, Gurda BL, Engiles JB, et al. Multiple recombinant adeno-associated viral vector serotypes display persistent *in vivo* gene expression in vector-transduced rat stifle joints. *Hum Gene Ther Methods* 2013;24:185–194.
13. Guy J, Qi X, Muzyczka N, et al. Reporter expression persists 1 year after adeno-associated virus-mediated gene transfer to the optic nerve. *Arch Ophthalmol* 1999;117:929–937.
14. Vincent KR, Conrad BP, Fregly BJ, et al. The pathophysiology of osteoarthritis: a mechanical perspective on the knee joint. *PM R* 2012;4:S3–9.
15. Goodrich LR, Nixon AJ. Medical treatment of osteoarthritis in the horse—a review. *Vet J* 2006;171:51–69.
16. McCarty DM, Monahan PE, Samulski RJ. Self-complementary recombinant adeno-associated virus (scAAV) vectors promote efficient transduction independently of DNA synthesis. *Gene Ther* 2001;8:1248–1254.
17. McCarty DM, Fu H, Monahan PE, et al. Adeno-associated virus terminal repeat (TR) mutant generates self-complementary vectors to overcome the rate-limiting step to transduction *in vivo*. *Gene Ther* 2003;10:2112–2118.
18. Watson Levings R, Broome TA, Smith AD, et al. Gene therapy for osteoarthritis: pharmacokinetics of intra-articular self-complementary adeno-associated virus interleukin-1 receptor antagonist delivery in an equine model. *Gene Ther Dev* 2018;29:90–100.
19. Li C, Diprimio N, Bowles DE, et al. Single amino acid modification of adeno-associated virus capsid changes transduction and humoral immune profiles. *J Virol* 2012;86:7752–7759.
20. Frisbie DD, Ghivizzani SC, Robbins PD, et al. Treatment of experimental equine osteoarthritis by *in vivo* delivery of the equine interleukin-1 receptor antagonist gene. *Gene Ther* 2002;9:12–20.
21. Ishihara A, Bartlett JS, Bertone AL. Inflammation and immune response of intra-articular serotype 2 adeno-associated virus or adenovirus vectors in a large animal model. *Arthritis* 2012;2012:735472.
22. Ortvad K, Wagner B, Calcedo R, et al. Humoral and cell-mediated immune response, and growth factor synthesis after direct intraarticular injection of rAAV2-IGF-I and rAAV5-IGF-I in the equine middle carpal joint. *Hum Gene Ther* 2015;26:161–171.
23. Keegan KG, MacAllister CG, Wilson DA, et al. Comparison of an inertial sensor system with a stationary force plate for evaluation of horses with bilateral forelimb lameness. *Am J Vet Res* 2012;73:368–374.
24. Keegan KG, Wilson DA, Kramer J, et al. Comparison of a body-mounted inertial sensor system-based method with subjective evaluation for detection of lameness in horses. *Am J Vet Res* 2013;74:17–24.
25. Winter MD. The basics of musculoskeletal magnetic resonance imaging: terminology, imaging sequences, image planes, and descriptions of basic pathologic change. *Vet Clin North Am Equine Pract* 2012;28:599–616.
26. Smith AD, Morton AJ, Winter MD, et al. Magnetic resonance imaging scoring of an experimental model of post-traumatic osteoarthritis in the equine carpus. *Vet Radiol Ultrasound* 2016;57:502–514.
27. Roemer FW, Kassim Javaid M, Guermazi A, et al. Anatomical distribution of synovitis in knee osteoarthritis and its association with joint effusion assessed on non-enhanced and contrast-enhanced MRI. *Osteoarthritis Cartilage* 2010;18:1269–1274.
28. Sun J, Hua B, Chen X, et al. Gene delivery of activated Factor VII using alternative adeno-associated virus serotype improves hemostasis in hemophilic mice with FVIII inhibitors and adeno-associated virus neutralizing antibodies. *Hum Gene Ther* 2017;28:654–666.
29. Elsaid KA, Zhang L, Shaman Z, et al. The impact of early intra-articular administration of interleukin-1 receptor antagonist on lubricin metabolism and cartilage degeneration in an anterior cruciate ligament transection model. *Osteoarthritis Cartilage* 2015;23:114–121.
30. Zhang X, Schwarz EM, Young DA, et al. Cyclooxygenase-2 regulates mesenchymal cell differentiation into the osteoblast lineage and is critically involved in bone repair. *J Clin Invest* 2002;109:1405–1415.
31. Geusens P, Emans PJ, de Jong JJ, et al. NSAIDs and fracture healing. *Curr Opin Rheumatol* 2013;25:524–531.
32. Claes L, Recknagel S, Ignatius A. Fracture healing under healthy and inflammatory conditions. *Nat Rev Rheumatol* 2012;8:133–143.
33. Matzelle MM, Gallant MA, Condon KW, et al. Resolution of inflammation induces osteoblast function and regulates the Wnt signaling pathway. *Arthritis Rheum* 2012;64:1540–1550.
34. Chang J, Liu F, Lee M, et al. NF- κ B inhibits osteogenic differentiation of mesenchymal stem cells by promoting β -catenin degradation. *Proc Natl Acad Sci U S A* 2013;110:9469–9474.
35. Arend WP, Welgus HG, Thompson RC, et al. Biological properties of recombinant human monocyte-derived interleukin 1 receptor antagonist. *J Clin Invest* 1990;85:1694–1697.
36. Arend WP. The balance between IL-1 and IL-1Ra in disease. *Cytokine Growth Factor Rev* 2002;13:323–340.

Received for publication August 8, 2017;
accepted after revision June 1, 2018.

Published online: June 4, 2018.